Construction by Contour Crafting using Sulfur Concrete with Planetary Applications

Behrokh Khoshnevis, Xiao Yuan, Behnam Zahiri, Bin Xia

Department of Industrial and Systems Engineering, University of Southern California, California, CA 90089

Abstract

This paper reports on the experiments with the Contour Crafting Automated Construction process using sulfur concrete as the choice of construction material. Sulfur concrete has numerous terrestrial applications and is potentially an ideal construction material for planetary construction. On Mars, sulfur can be found in abundance and the range of temperature variation on the planet is within the safe zone for the structures to be built and survive over reasonable length of time with sulfur concrete. Several experiments have been performed at centimeter and meter scales. A FEA simulation model for the behavior of sulfur concrete based structures has been developed. Experimental results were compared with the results of simulation.

Key words: additive manufacturing, Contour Crafting, sulfur concrete, planetary.

Introduction

The Sulfur Concrete Contour Crafting (SCCC) is a layer-based 3D printing technology which uses sulfur concrete. Additive manufacturing has the advantage of having a low-cost, high strength, high acid/salt resistance and durable structure at high speed [1]. The SCCC is equipped with a 6-axis robot and a universal sulfur concrete extruder which can automatically collect local construction material and build on complex terrain. This technology has the potential to construct in outer spaces and in environments such as Mars or Moon, since both are abundant in sulfur. [2]

In the SCCC process the sulfur concrete composite materials (elemental sulfur, sulfur modifier, coarse aggregate and fine aggregate) are pre-melted and mixed at 150C, and are kept in the reservoir for one hour until the elemental sulfur are modified [1]. Then the well-prepared sulfur concrete is deposited by a special mixer/extruder fixed on a 6-axis robot. Sulfur concrete is deposited on the previous layer to the calculated path and cures in less than 10 minutes. After 24 hours, the construction made by sulfur concrete reaches its highest strength.

Background

In an earlier part of this NASA supported project a new mini-size auger with piezo vibration was developed to investigate the possibility of reliably extruding sulfur concrete. As it is shown in Figure 1, dry sulfur and Martian regolith simulant in the funnel were pushed downward through a nozzle by a rotating auger while sulfur was being melted by electric heaters. The nozzle head formed the shape of the exiting sulfur concrete and built smooth surfaces and edges. To increase the bonding strength of the layer, a feature was added to the nozzle to produce an interlocking profile for successive layers [3].

To automatically counteract the bridging effect during the extruding process a vertical vibration was induced by a piezo transducer to the auger and a horizontal vibration piezo was added to the end of the extruder shown in Figure 1. These two piezo actuators partially alleviated friction during the extrusion process.
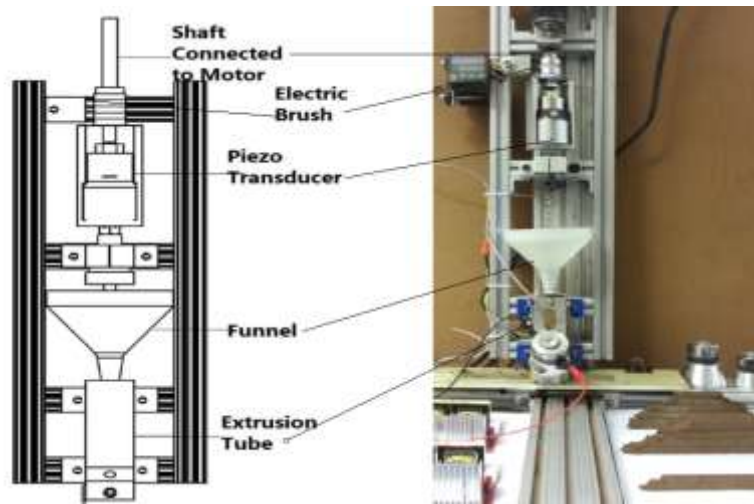
Figure 1: Schematic of Mini-size auger extruder

To improve the efficiency of heating, an experiment was carried out by pre-heating mixed sulfur and Martian regolith simulant in water at 98℃ for half an hour. This dramatically improved the melting efficiency in the extrusion process as shown in Figure 2. In comparison to heating process in room temperature from melting temperature of sulfur at 115 C, pre-heating method further reduces the extrusion friction and improves the final surface of extruded Martian sulfur concrete. Of course use of water on Moon and Mars is problematic and other approaches such as the use of microwave for preheating may be considered. Figure 3 shows the Martian regolith dome built by this process.[3]
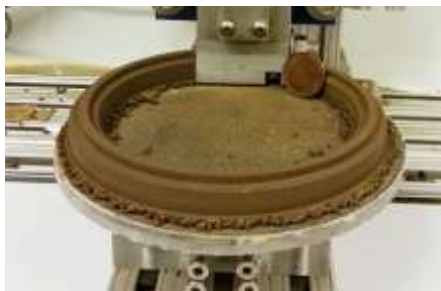

Figure 2: Extruded sample with smooth surface   *Figure 3: Martian regolith dome*

Although the surface quality of the extruded layer has been optimized, the rotation torque has been excessive. Also, auger blade gets damaged when it is being used for 50 hours at a low temperature, especially on the upper part of the nozzle. As shown in Figure 4, while the auger blade initially had a width of 3mm, it became 0.3mm due to abrasion caused by hard aggregate in regolith stimulant. Silicon dioxide makes half of the content of the regolith stimulants, having durability measuring between 4500~9500 MPa.

Figure 4: Auger worn-out during experiment

The new approach

To ensure durability, stability and reliability of sulfur concrete extruder, a new universal concrete extruder was conceived and examined. As shown in Figure 5, the new mixer/extruder combination mechanism was devised in which the entire mixing and extrusion chambers were precisely heated. In contrast with the previous auger extruder, the stage-wise mechanisms on the upper sections move the material downward while a special extruder at the end of the nozzle provides the main extrusion force. In addition, the mixture is completely melted before entering the nozzle and as such its friction with the walls of the nozzle is far less than the mixture at the ambient temperature or even pre-heated mixture. Besides these two alterations, an aluminum extender end which also acts as heat sink is added to the outlet of the nozzle to lower the temperature of the exiting material quickly. Fuzzy logic control is employed to control the DC motor that mixes the material and moves it downward through the nozzle. Although this control system has proven to be more consistent and accurate, the volume of extrusion tube limits the maximum length of extrusion.
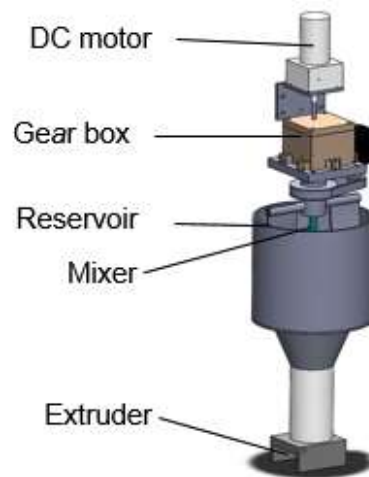

Figure 5: The mixer/extruder assembly

A continuous process for feeding the nozzle assembly was developed on the basis of the above approach. Figure 6 shows the new fabrication process concept where raw aggregate and dry sulfur are transported into a hopper installed on top of the nozzle. The hopper heats and mixes the material at 150 C. As the sulfur concrete mixture in the reservoir gets consumed, the robot moves the extrusion system along with its reservoir under the silo outlet at the refill station.
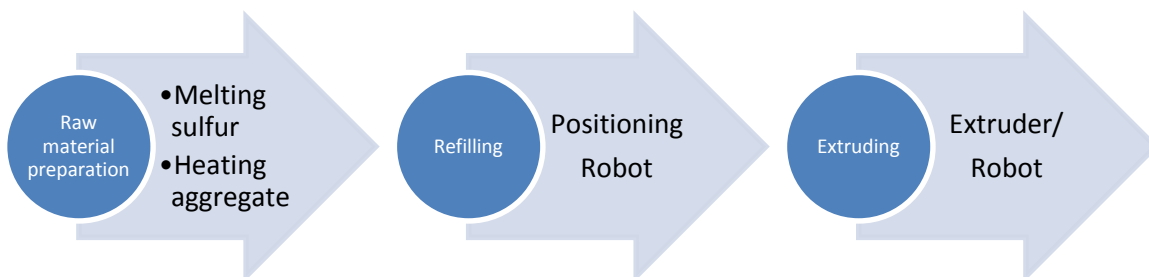

Figure 6: The construction process

For the construction of full-scale structures, a large industrial robot is being used in the Contour Crafting Laboratory. The robot (KUKA brand) consists of six rotational actuators which provide six degrees of freedom. One of the most important advantages of using such robot over a gantry robot is that for a given size of structure the gantry has to be designed in such a way that it can contain the structure within its work envelope. However,

a joint robot such as the KUKA robot used in this experiment can be mounted on top of a rover to eliminate the size restriction.

Figure 7: Sulfur concrete contour crafting robot

Figure 8: Three layers extrusion sample

Building 3D dome structures requires following more complicated pathways than straight or circular lines. For a stationary robot (not mounted on a rover) the position of starting layer in the global coordinate system must be selected in such a way that the whole dome structure falls completely within the robot workspace. Different shapes and geometries can be selected for the dome-like structures. One of the candidates for the 3D dome structure is depicted in Figure 9. For this structure inclined layers are built consecutively such that each layer has a slight angle with respect to the horizontal plane.
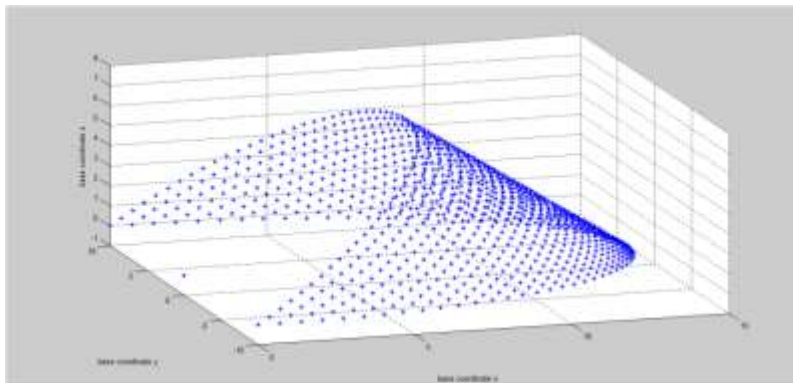

Figure 9: Tool path coordinates for dome-like structure

Other patterns to achieve dome-like structures are also being considered. For instance, patterns which inherit geometric advantages of domes and cones can be used to build optimum structures by horizontal, rather than inclined, layering method. We plan to investigate relevant merits of different geometric structures in order to determine the optimum shape such that each layer has sufficient support and the whole structure shows robust stability and strength.

Sulfur concrete extrusion study

Workability is the most important property of molten sulfur concrete, which not only affects the transportation and extrusion but also the strength and surface quality of the final product. Bartos [4] explained workability with several fundamental characteristics such as viscosity, mobility, internal friction, pumpability, segregation, bleeding, formability and finishability.

In Contour Crafting with sulfur concrete, mobility and pumpability of molten sulfur concrete affect the extrudability of the mix. While, the formability and finishability affect the strength and surface quality of extruded strucutres. Unfortunately, the molten sulfur concrete with high mobility and pumpability always has

poor formability and finished quality and this is the difficult contradiction in this project. So, exploring the appropriate sulfur concrete for the two sets of contradicting properties and developing the effective nozzle for forming sulfur concrete are the two main tasks of this project [4].
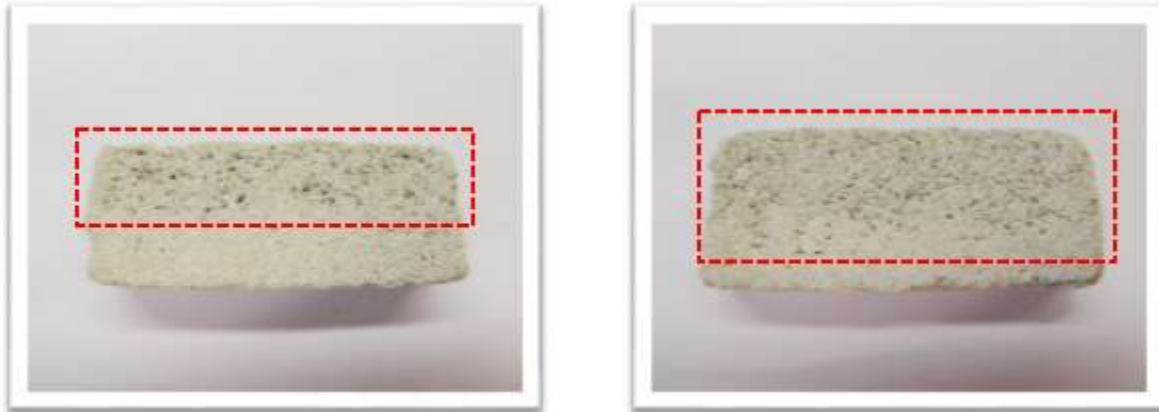
The performance of the extrusion process varies considerably with different proportions of sulfur in sulfur concrete. When sulfur proportion in the mix is high the sulfur concrete has low viscosity, which makes it easy to extrude. However, low viscosity also causes the problem of having high slump and leakage. On the other hand, low proportion of sulfur lowers the slump, but a low viscosity mixture is hard to extrude as it always sticks to extrusion barrel and internal mechanisms.

To explore the significant factors that may influence the extrusion process a 2k factorial experiment was designed based on temperature at different stages, proportion of sulfur and extrusion/moving speed as shown in Table 1.

Table 1: A 2k factorial design on extruding process

Factors	Level -	Level +
Sulfur Proportion	30 wt%	35 wt%
Sulfur Concrete Temperature	140 C	150 C
Extruder Temperature	150 C	160 C
Extrusion Rate	3 kg/min	5 kg/min
Extrusion Rate	3 kg/min	5 kg/min

When the sulfur concrete does not stick to the inner wall of the barrel and with the force of gravity flows smoothly to the lower sections of the nozzle, the experiment shows that the extruder temperature and extrusion rate have little effect on the extrusion process.
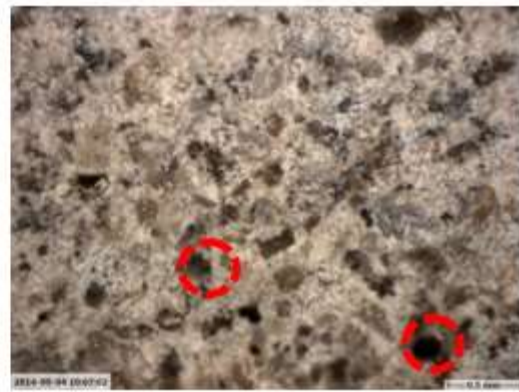

(a) Sample built in 140C   *(b) Sample built in 150C*

Figure 10: Extrusion process with different sulfur cement temperature

In the experiment it is obvious that the mixture at 150C has less viscosity and better flow rate. Some extrusion cross-sections are observed under optical microscope, as shown in Figures 10 and 11. The porous structure is more equally distributed in the sample built at 150 C as shown in (b), while most of porous structure is shown in (a) as sample built in 140C. It is deduced that sulfur in mixture at 150C took longer for the curing process and sank into the lower region of parts by the force of gravity. The uneven sulfur content between upper and lower parts may considerably reduce the strength of multi-layer structures.
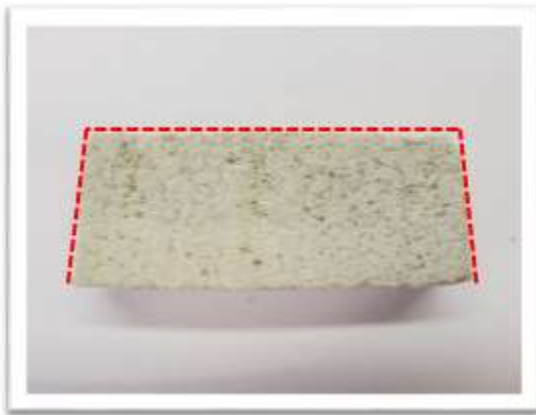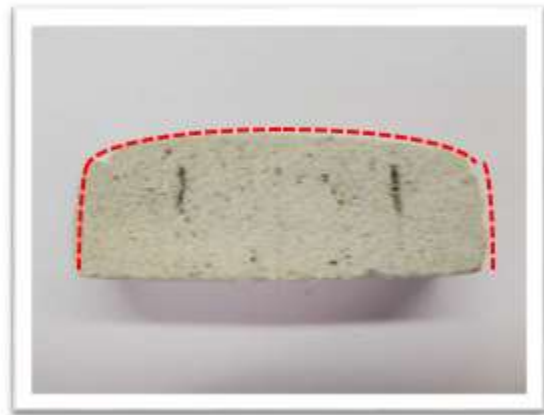
(a) Sample built in 140C   *(b) Sample built in 150C*

Figure 11: Extrusion process with different sulfur cement temperature

Sulfur plays the role of binder in solidified sulfur concrete and the role of lubricant during the extrusion process. By increasing sulfur proportion the viscosity of sulfur cement decreases considerably, therefore, the liquidity increases. Compared to the 30 wt% sulfur concrete samples, the 35 wt% sulfur concrete is saturated with sulfur and hence the porosity level is not significant. However, the plasticity of 35 wt% sulfur cement in the molten state is less than that of 30 wt% sulfur concrete. This may explain the reason behind the round shapes of both edges and top surface of the sample on the right in Figure 12. In such cases it is especially necessary to add side trowels behind the nozzle to keep the extruded surface smooth.

(a) Sample with 30wt% sulfur   *(b) Sample with 35wt% sulfur*

Figure 12: Extrusion process with different mixture temperature

(a) Sample with 30wt% sulfur   *(b) Sample with 35wt% sulfur*

Figure 13: Extrusion process with different mixture temperature

From Figure 13 it is clear that the microscopic characteristics of the two samples are different. The size of microscopic holes in the two samples differs greatly. Porosity directly impacts the strength of the structures made with these materials. By choosing the appropriate weight ratio for sulfur in the mixture, the porosity can be decreased.

Finite Element Analysis

A finite element analysis for the deformation behavior of sulfur concrete immediately after extrusion was conducted by using the finite element code. The details of analysis are given below.

a) Description of constitutive model and selection of material parameters

Mohr Coulomb Plasticity model, provided within the material library of ABAQUS, was selected for the description of the rheological behavior of uncured sulfur concrete right after extrusion. According to Mohr-Coulomb model, failure in the element begins when the shear stress in a material reaches a threshold that depends linearly on the normal stress in the same plane. By plotting Mohr's circle for states of stress at failure in the plane of the maximum and minimum principal stresses, the failure line is defined as the best straight line that touches these Mohr's circles as shown in Figure 13 [5].
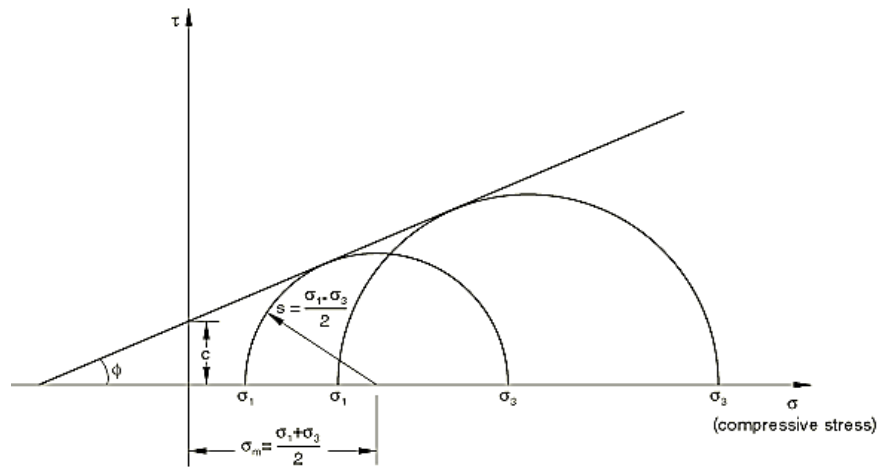

Figure 13: Mohr-Coulomb failure model [5]

According to figure 13, the Mohr-Coulomb model is defined by [5]

$$\tau = c - \sigma \tan\phi \qquad (1)$$

Where σ would have a positive sign in tension and a negative sign in compression. In Equation (1) ϕ is the friction angle and c is the cohesion of the material. With some manipulation in Equation (1), the Mohr-Coulomb model can be written as

$$s + \sigma_m \sin\phi - c\cos\phi = 0 \qquad (2)$$

This model can also be written in the general form as:

$$F = R_{mc}q - p\tan\phi - c = 0 \qquad (3)$$

Where

$$R_{mc}(\Theta,\phi) = \frac{1}{\sqrt{3}\cos\phi}\sin\left(\Theta + \frac{\pi}{3}\right) + \frac{1}{3}\cos\left(\Theta + \frac{\pi}{3}\right)\tan\phi \qquad (4)$$

The essential components of the Mohr-Coulomb model are described below:
- Friction angle: In Equation (1-4), ϕ is the friction angle which is the slope of the Mohr-Coulomb yield surface in the $p\_R_{mc}q$ stress plane (see Figure 14), which is commonly referred to as the friction angle of the material and can depend on temperature and predefined field variables.
- Dilation angle measured in the $p\_R_{mc}q$ plane at high confining pressure and can depend on temperature and predefined field variables.
- Cohesion: In Equation (1-4) c is the cohesion of the material.

1765

The geometry of the yield surface in the deviatoric plane is controlled by the friction angle ϕ as shown in Figure 14. The range for friction angle variation is from $0 \le \phi < 90$. In the case of $\phi = 0$, the Mohr-Coulomb model reduces to the pressure-independent Tresca model with a perfectly hexagonal deviatoric section. In the case of $\phi = 90$ the Mohr-Coulomb model reduces to the "tension cut-off" Rankine model with a triangular deviatoric section and $R_{mc} = \infty$ [5].
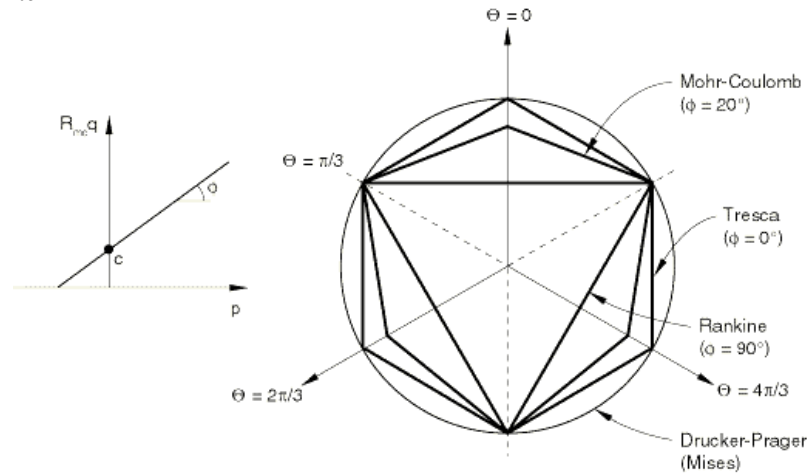

Figure 14: Mohr-Coulomb yield surface in meridional and deviatoric planes [5]

b) Geometry and boundary conditions
The geometry of the specimen is shown in Figure 15. Only one half of the specimen could also be modeled for the analysis to get the results since the deformation analysis of the concrete has axisymmetric nature. The specimen was meshed using four-node axisymmetric elements. The surface beneath the specimen was modeled as a rigid body with friction interaction with the model.
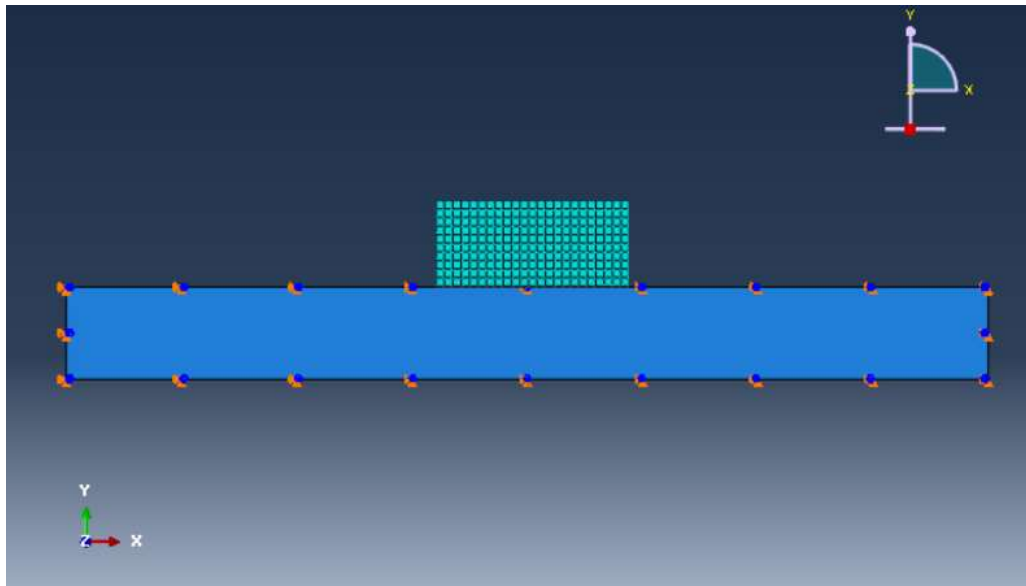

Figure 15: The geometry of the specimen and the initial mesh used to implement the finite element analysis.

c) Numerical results and a comparison with the experimental data
The relative geometrical deformation from the FEA model was obtained and compared to the experimental results (Figure 16, 17). By changing the viscosity in each experiment and using an iterative recursive curve

1766

fitting method, we are able to obtain an FEA model for uncured sulfur concrete which can predict the deformation of the extruded mixture as a function of viscosity.
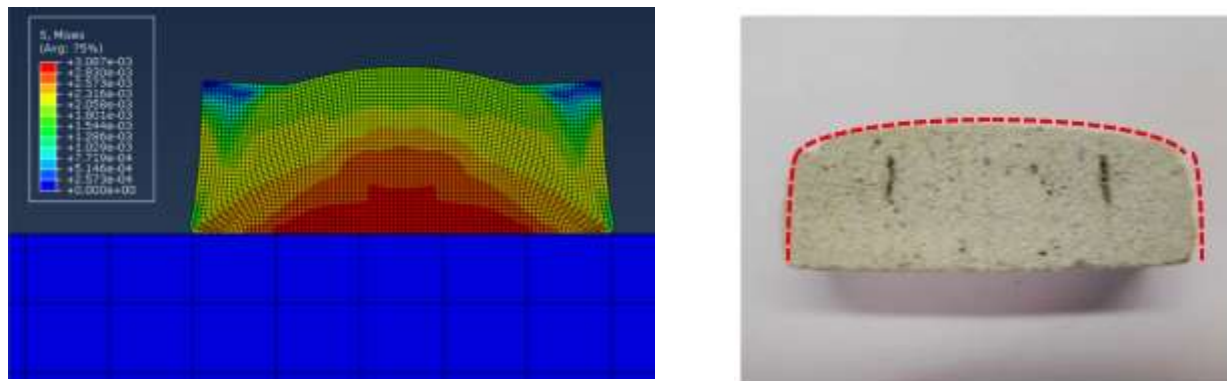

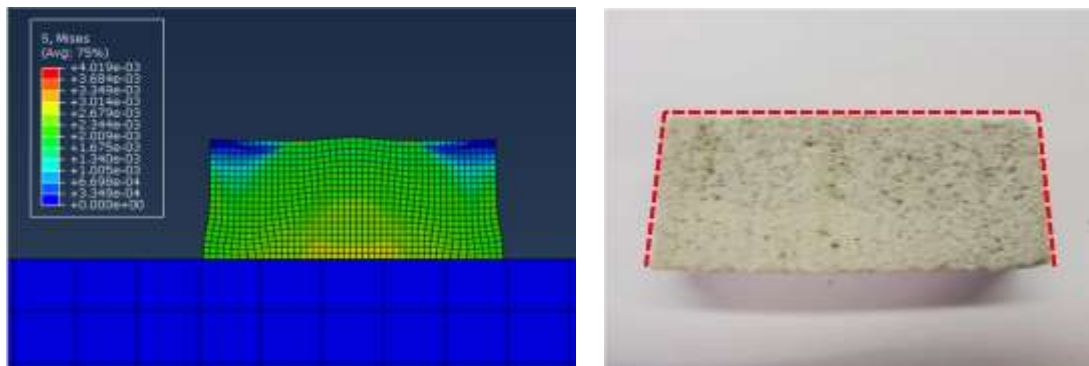*Figure 16: The Mohr-Coulomb based FEA model and the extruded sample 35%wt*

Figure 17: The Mohr-Coulomb based FEA model and the extruded sample 30%wt

Figures 16 and 17 show the FEA models versus the experimental samples. The essential parameters in the Mohr-Coulomb model is different for the two samples with different sulfur contents. The appropriate friction coefficients between the samples and the base were found by comparing the experimental results with the FEA results so that the friction coefficients were in the best agreement between the predicted and experimental deformation patterns.

6. Conclusion

Experimental samples was developed using a novel mixer/extrusion system. The mechanism was proven to be durable and stable after more than 500 hour's work. The extrusion experiment showed that the temperature and proportion of composite influenced the final shape of extrusion. Higher extrusion temperature made the samples less porous. Less sulfur proportion improved the shape and surface of the extrudate but increased the porosity. Relative deformation of different samples with different proportions of ingredients were studied. The experimental results obtained were compared with those found from a FEA analysis. A constitutive model based on Mohr Coulomb Plasticity model was used for the FEA calculations. The simulations based on the FEA model show the potential for improving the deformations of sulfur concrete after extrusion.

Acknowledgement

Reference

[1]   A.-M. O. Mohamed and M. El-Gamal, Sulfur concrete for the construction industry: a sustainable development approach. J. Ross Publishing, 2010.

[2]   B. Khoshnevis, M. Bodiford, K. Burks, E. Ethridge, D. Tucker, W. Kim, H. Toutanji, and M. Fiske, "Lunar contour crafting—a novel technique for ISRU-based habitat development," Autom. Constr., vol. 13(1), no. January, pp. 5–19, 2004.

[3]   B. Khoshnevis, M. Thangavelu, X. Yuan, and J. Zhang, "Advances in Contour Crafting Technology for Extraterrestrial Settlement Infrastructure Buildup," AIAA, vol. 5438, pp. 10–12, 2013.

[4]   P. Bartos, Fresh concrete: properties and tests. Elsevier, 2013.

[5]   ABAQUS (2011) `ABAQUS 6.11 Analysis User's Manual'. Online Documentation: Dassault Systèmes.

[6]   Menétrey, Ph., and K. J. Willam, "Triaxial Failure Criterion for Concrete and its Generalization," ACI Structural Journal, vol. 92, pp. 311–318, May/June 1995.